Inorg. Chem. **2005**, *44*, 316–324

Oxidative Dissolution of Copper and Zinc Metal in Carbon Dioxide with *tert*-Butyl Peracetate and a *β*-Diketone Chelating Agent

Pamela M. Visintin,[†] Carol A. Bessel,*[,‡] Peter S. White,[†] Cynthia K. Schauer,*[,†] and Joseph M. DeSimone*[,†,§]

Department of Chemistry, University of North Carolina at Chapel Hill, Chapel Hill, North Carolina 27599-3290, Department of Chemical Engineering, North Carolina State University, Raleigh, North Carolina 27695-7565, and Department of Chemistry, Villanova University, 800 Lancaster Avenue, Villanova, Pennsylvania 19085

Received February 22, 2004

A series of *β*-diketone ligands, $R^1COCH_2COR^2$ [tmhdH ($R^1 = R^2 = C(CH_3)_3$); tfacH ($R^1 = CF_3$; $R^2 = CH_3$); hfacH ($R^1 = R^2 = CF_3$)], in combination with *tert*-butyl peracetate (*t*-BuPA), have been investigated as etchant solutions for dissolution of copper metal into carbon dioxide solvent. Copper removal in CO_2 increases in the order tfacH < tmhdH < hfacH. A study of the reactions of the hfacH/*t*-BuPA etchant solution with metallic copper and zinc was conducted in three solvents: $scCO_2$ (supercrical CO_2); hexanes; CD_2Cl_2. The etchant solution/metallic zinc reaction produced a diamagnetic Zn(II) complex, which allowed NMR identification of the *t*-BuPA decomposition products as *tert*-butyl alcohol and acetic acid. Gravimetric analysis of the amount of zinc consumed, together with NMR studies, confirmed the 1:1:2 Zn:*t*-BuPA:hfacH reaction stoichiometry, showing *t*-BuPA to be an overall two-electron oxidant for Zn(0). The metal-containing products of the copper and zinc reactions were characterized by elemental analysis, IR spectroscopy, and, as appropriate, NMR spectroscopy and single-crystal X-ray diffraction [*trans*-$M(hfac)_2(H_2O)(CH_3CO_2H)$ (**1**, M = Cu; **2**, M = Zn)]. On the basis of the experimental results, a working model of the oxidative dissolution reaction is proposed, which delineates the key chemical variables in the etching reaction. These *t*-BuPA/hfacH etchant solutions may find application in a CO_2-based chemical mechanical planarization (CMP) process.

Introduction

The fabrication of copper interconnect devices for logic circuits in the microelectronics industry requires a fundamental understanding of copper chemical mechanical planarization (CMP) technologies.[1−3] CMP is a process which uses a slurry containing chemicals and abrasive particles to oxidize, chelate, and remove the copper metal overburden while the polishing pad mechanically removes the surface materials until a flat surface is achieved. Current CMP processes use water as the solvent, leading to technical and environmental difficulties. As feature sizes approach line widths below 150 nm and aspect ratios greater than 3, the high surface tension of water makes it difficult to completely remove aqueous solvents from the porous low-*k* interlayer dielectric materials, leading to higher than desired dielectric constants. Furthermore, porous materials do not have sufficient mechanical strength to withstand the destructive forces associated with high surface tension liquids such as water,[4] resulting in image collapse of the structures.

Research focused on enabling a liquid and/or supercritical (sc) CO_2 technology platform for microelectronics applications is responding to needs for solvent-compatible wafer processing and more environmentally benign replacements for organic and aqueous solvents.[5] Condensed CO_2 has desirable characteristics for CMP processing, including high surface wetting, extremely low viscosity, low surface tension, and a low dielectric constant. Additionally, condensed CO_2

* Authors to whom correspondence should be addressed. E-mail: carol.bessel@villanova.edu (C.A.B.); schauer@unc.edu (C.K.S.); desimone@unc.edu (J.M.D.).
[†] University of North Carolina at Chapel Hill.
[‡] Villanova University.
[§] North Carolina State University.

(1) Steigerwald, J. M.; Murarka, S. P.; Gutmann, R. J. *Chemical Mechanical Planarization of Microelectronic Materials*; John Wiley & Sons: New York, 1997.
(2) Singh, R. K.; Bajaj, R. *MRS Bull.* **2002**, *27*, 743.
(3) Hanazono, M.; Amanokura, J.; Kamigata, Y. *MRS Bull.* **2002**, *27*, 772.
(4) DeSimone, J. M. *Science* **2002**, *297*, 799.
(5) Weibel, G. L.; Ober, C. K. *Microelectron. Eng.* **2003**, *65*, 145.

10.1021/ic049765o CCC: $30.25
Published on Web 12/16/2004

is a very attractive solvent choice from an environmental perspective because it is readily available, nontoxic, nonflammable, and has the potential to be recycled. Recently, we reported that copper metal can be oxidized and chelated in CO_2 media using ethyl peroxydicarbonate (EPDC) as an oxidant with a β-diketone chelating agent (eq 1).[6] This observation, which builds upon extensive studies of vapor phase etching of copper metal and oxidized copper species with β-diketone chelating agents,[7−11] has opened the possibility of a CO_2-based CMP technology for copper. The CO_2 solution reaction medium and the soluble oxidant allow these etching reactions to be conducted at low temperatures relative to the vapor phase reactions.

$$\text{Cu(0)} \xrightarrow{\text{EPDC, }\beta\text{-diketone}} \text{bis}(\beta\text{-diketonato})\text{copper(II)} \quad (1)$$

The oxidant, EPDC, has several inherent limitations, including the lack of its availability from commercial sources, its highly toxic starting material (ethyl chloroformate), and its very high reactivity. This study examines reaction of a series of β-diketone ligands, $R^1COCH_2COR^2$ [tmhdH ($R^1 = R^2 = C(CH_3)_3$); tfacH ($R^1 = CF_3$; $R^2 = CH_3$); hfacH ($R^1 = R^2 = CF_3$)], in combination with *tert*-butyl peracetate (*t*-BuPA) as etchant solutions, for application in copper CMP in $scCO_2$. The oxidant, *t*-BuPA, was selected for this study due to its commercial availability, CO_2 solubility, efficiency, safe handling ability, and cost-effectiveness.

The reaction between metallic copper and zinc with the hfacH/*t*-BuPA etchant solution is examined in detail to identify the peroxy ester decomposition products and metal products of the reaction. The fact that the Zn(II) product is diamagnetic allows use of NMR spectroscopy to determine the reaction stoichiometry and to identify the *t*-BuPA decomposition products for the zinc reaction. The effect of solvent on the etching reaction is assessed by comparing reactions performed in conventional organic solvents (hexanes and CD_2Cl_2) with those conducted in $scCO_2$.[12] A working model of the oxidative dissolution reaction is proposed, which delineates the key chemical variables in the etching reaction.

Experimental Section

Materials and General Procedures. Copper powder (Alfa Aesar, APS 0.2−0.3 μm, 99.9%) was stored and handled in an argon-filled Vacuum Atmospheres glovebox. Copper coupons (99.999%, 0.1 mm thick), zinc coupons (99.999%, 0.1 mm thick), 1,1,1,5,5,5-hexafluoroacetylacetone (hfacH), 1,1,1-trifluoro-2,4-pentanedione (tfacH), 2,2,6,6-tetramethyl-3,5-heptanedione (tmhdH), *tert*-butyl peracetate (*t*-BuPA, 75 wt % in aliphatic hydrocarbons), $Cu(hfac)_2 \cdot H_2O$, and $Cu_2(O_2CCH_3)_4 \cdot 2H_2O$ were purchased from Aldrich and were used as received. Unless otherwise noted, all other solvents were purchased in reagent grade from commercial suppliers and used without further purification. Carbon dioxide (SFC/SFE grade) was supplied by Air Products. **Caution!** *Although we have experienced no difficulty with t-BuPA, this solution should be treated as potentially explosive and handled with care.*

Characterization Methods. Melting points were determined with an Electrothermal melting point apparatus. NMR spectra were recorded at room temperature on a Bruker Avance 400 MHz spectrometer. Chemical shifts are reported in parts per million (δ). ^1H and $^{13}C\{^1H\}$ NMR chemical shifts are referenced to the residual ^1H and $^{13}C\{^1H\}$ signals of the deuterated solvents. ^{19}F NMR resonances are reported using C_6F_6 ($\delta = -164.9$ from $CFCl_3$) as the internal reference. Infrared spectra were recorded using KBr pellets on a Bio-Rad FTS-7 spectrometer, in the 4000−500 cm^{-1} range. UV−visible spectroscopy was performed using a Perkin-Elmer Lambda 40 spectrophotometer in the range 190−860 nm. Elemental analyses were performed by Atlantic Microlab, Inc. (Norcross, GA).

Dissolution of Copper Metal in $scCO_2$. A 10-mL high-pressure 316 stainless steel sapphire-windowed view cell was employed for each reaction. The *t*-BuPA (0.07 mL, 3.5×10^{-4} mol), a β-diketone chelating agent (6.9×10^{-4} mol), and a copper coupon (0.022 g, 3.5×10^{-4} mol, contained in a glass holder) were placed in the cell. The cell was charged with CO_2 (214 ± 3 bar, 40 ± 2 °C), and the mixture was stirred for 20 h. The cell was then vented, and the coupon was rinsed with hexanes, dried, and weighed. The number of monolayers (m) of copper removed was calculated from the weight loss, area of the coupon × 2 (for a two-sided coupon), and the atomic radius of copper (r).[13] The average dissolution rate was then calculated using the total reaction time (t) (eq 2).

$$\text{rate} = \frac{mr}{t} \quad (2)$$

Reaction of Metallic Copper with *t*-BuPA and hfacH in Hexanes. To a suspension of copper powder (0.095 g, 1.5×10^{-3} mol) in 10 mL of hexanes at 40 °C under nitrogen were added *t*-BuPA (0.45 mL, 2.3×10^{-3} mol) and hfacH (0.53 mL, 3.8×10^{-3} mol). The reaction mixture was stirred for 4.5 d, yielding a homogeneous dark green solution. The solution was cooled, and on slow evaporation of the solvent, green crystals of *trans*-$Cu(hfac)_2(H_2O)(CH_3CO_2H)$ (**1**) suitable for X-ray diffraction measurements were formed. The crystalline solid was filtered, washed with pentane (5 mL), and dried under vacuum (0.69 g, 84% yield based on copper metal): mp 107−112 °C; IR (KBr) 3568 (m) $\nu(H_2O)$, 1718 (w) $\nu_{AcOH}(C{=}O)$, 1646 (s) $\nu(C{\cdots}O)$, 1617 (m) $\nu(C{\cdots}C)$, 1563 (m) $\nu(C{\cdots}O) + \delta_{hfac}(CH)$, 1537 (m), 1470 (s), 1357 (m) $\nu(C{\cdots}C) + \nu(CF_3)$, 1258 (vs) $\nu(CF_3)$, 1223 (s) $\nu_{AcOH}(C{-}O) + \delta_{AcOH}(OH)$, 1208 (sh), 1150 (vs) $\beta_{hfac}(CH)$, 1109 (m), 809(s) $\gamma_{hfac}(CH) + \nu(C{-}CF_3)$, 772 (w) and 748 (m) $\nu(C{-}CF_3)$, 681 (s), 599 (s), 532 (m) cm^{-1}. Anal. Calcd for $C_{12}H_8O_7F_{12}Cu$: C, 25.93; H, 1.45; F, 41.03. Found: C, 25.42; H, 1.42; F, 41.61. The difference between the calculated and observed elemental analysis is likely due to an impurity of $Cu(hfac)_2(H_2O)$. Attempts to separate these complexes by recrystallization were unsuccessful.

Reaction of Metallic Zinc with *t*-BuPA and hfacH in Hexanes. A zinc coupon (0.098 g, 1.5×10^{-3} mol) was added to *t*-BuPA

(6) Bessel, C. A.; Denison, G. M.; DeSimone, J. M.; DeYoung, J.; Gross, S.; Schauer, C. K.; Visintin, P. M. *J. Am. Chem. Soc.* **2003**, *125*, 4980.
(7) Sekiguchi, A.; Kobayashi, A.; Koide, T.; Okada, O.; Hosokawa, N. *Jpn. J. Appl. Phys., Part 1* **2000**, *39*, 6478.
(8) Farkas, J.; Chi, K. M.; Hampden-Smith, M. J.; Kodas, T. T.; Dubois, L. H. *Mater. Sci. Eng., B* **1993**, *17*, 93.
(9) Jain, A.; Kodas, T. T.; Hampden-Smith, M. J. *Thin Solid Films* **1995**, *269*, 51.
(10) George, M. A.; Hess, D. W.; Beck, S. E.; Ivankovits, J. C.; Bohling, D. A.; Lane, A. P. *J. Electrochem. Soc.* 1995.
(11) Steger, R.; Masel, R. *Thin Solid Films* **1999**, *342*, 221.
(12) Although this reaction does occur in liquid CO_2, the set of conditions used in this study are in the $scCO_2$ regime (see ref 6).
(13) *Chemistry: WebElements Periodic Table: Professional Edition: Copper: radii*; http://www.webelements.com/webelements/elements/text/Cu/radii.html (accessed Oct 2003).

(0.45 mL, 2.3×10^{-3} mol) and hfacH (0.53 mL, 3.8×10^{-3} mol) in 10 mL of hexanes at 40 °C under nitrogen. The coupon began to dissolve within 30 min and was completely dissolved within 2 h. The pale yellow solution was stirred for 24 h and cooled. Upon slow evaporation of the solvent, white crystals of *trans*-Zn(hfac)$_2$(H$_2$O)(CH$_3$CO$_2$H) (**2**) suitable for X-ray diffraction measurements were formed. The crystals were isolated by filtration, washed with hexanes (3×5 mL) and pentane (3×5 mL), and dried in vacuo (0.40 g, 50% yield based on zinc metal). Elemental analysis was fit to a 1:1 ratio of complexes *trans*-Zn(hfac)$_2$(H$_2$O)(CH$_3$CO$_2$H) (**2**) and Zn(hfac)$_2$·2H$_2$O. ^{1}H NMR spectroscopy further supports this 1:1 ratio. Attempts to separate these complexes by recrystallization were unsuccessful: mp 128−133 °C; IR (KBr) 3482 (br) ν(H$_2$O), 1733 (w) ν_{AcOH}(C=O), 1646 (vs) ν(C···O), 1615 (m) ν(C··· C), 1566 (s) ν(C···O) + δ_{hfac}(CH), 1540 (s), 1489 (vs), 1459 (s), 1349 (m) ν(C···C) + ν(CF$_3$), 1262 (vs) ν(CF$_3$), 1225 (vs) ν_{AcOH}(C−O) + δ_{AcOH}(OH), 1202 (sh), 1148 (vs) β_{hfac}(CH), 1097 (m), 808 (vs) γ_{hfac}(CH) + ν(C−CF$_3$), 773 (m) and 745 (s) ν(C−CF$_3$), 670 (vs), 591 (vs), 527 (s) cm^{-1}; ^{1}H NMR (400 MHz, acetone-d_6) δ 1.95 (s, 3H, C*H*$_3$), 5.93 (s, 4H, C*H*); ^{13}C{^{1}H} NMR (400 MHz, acetone-d_6) δ 20.6 (s, *C*H$_3$), 88.6 (s, *C*H), 118.5 (q, $J = 285.9$ Hz, *C*F$_3$), 173.0 (s, *C*=O), 178.8 (q, $J = 33.7$ Hz, *C*O); ^{19}F NMR (400 MHz, acetone-d_6, δ vs C$_6$F$_6$) δ −77.7 (s, C*F*$_3$). Anal. Calcd for C$_{12}$H$_8$O$_7$F$_{12}$Zn + C$_{10}$H$_6$O$_6$F$_{12}$Zn (1:1): C, 24.62; H, 1.32; F, 42.49. Found: C, 24.26; H, 1.31; F, 42.32.

Reaction of Copper with *t*-BuPA. To a suspension of copper powder (0.095 g, 1.5×10^{-3} mol) in 10 mL of absolute EtOH at 40 °C under nitrogen was added *t*-BuPA (0.45 mL, 2.3×10^{-3} mol). A dark blue/turquoise mixture resulted immediately. The reaction mixture was stirred for approximately 4.5 d, and then the excess copper solid was filtered off. The solvent was then removed, and the crude product was washed with hexanes (3×5 mL) and pentane (2×5 mL) and then dried under vacuum to afford Cu$_2$(O$_2$CCH$_3$)$_4$·2H$_2$O (**3**) (0.082 g, 28% yield based on copper metal). Crystals suitable for X-ray diffraction measurements were grown by vapor diffusion of toluene into the solution of **3** in absolute EtOH: mp 234−237 °C (dec); IR (KBr) 3473 (s) ν(H$_2$O), 3371 (s) ν(H$_2$O), 1602 (vs) ν_{as}(COO), 1422 (vs) ν_s(COO), 1355 (m) δ_s(CH$_3$), 1052 (m) ρ(CH$_3$), 943 (vw) ν(C−CH$_3$), 691 (s) δ_s(COO), 628 (s) ρ(COO), 526 (w) ρ(H$_2$O) cm^{-1}. Anal. Calcd for C$_8$H$_{16}$O$_{10}$Cu$_2$: C, 24.07; H, 4.03; O, 40.07. Found: C, 24.67; H, 4.31; O, 40.44.

The above procedure was conducted using a copper coupon (96.3 mg) to confirm the stoichiometry of the reaction on the basis of the moles of copper consumed/mol of dinuclear **3** produced. The remaining copper coupon was washed with EtOH and hexanes, dried under vacuum, and weighed. Approximately 41.3 mg (0.650 mmol) of copper was consumed and 129 mg (0.325 mmol) of **3** was produced. The molar ratio of Cu(0):**3** indicates a 1:2 (Cu:*t*-BuPA) stoichiometry in the EtOH reaction.

The above procedure using copper powder was also conducted using hexanes as a solvent rather than absolute EtOH. After 24 h of stirring, no reaction was apparent for either the solution or the suspended copper solid. The solid was then filtered out and washed twice with hexanes and finally with EtOH. The EtOH wash resulted in a blue/turquoise solution. Upon removal of solvent, a trace of blue solid resulted, which was identified as **3** by IR spectroscopy.

Reaction of Cu$_2$(O$_2$CCH$_3$)$_4$·2H$_2$O (3) with hfacH in Hexanes or scCO$_2$. To a suspension of Cu$_2$(O$_2$CCH$_3$)$_4$·2H$_2$O (**3**) (0.095 g, 1.5×10^{-3} mol) in 10 mL of hexanes at 40 °C under nitrogen was added hfacH (0.53 mL, 3.8×10^{-3} mol). A green mixture resulted immediately. This reaction mixture was stirred for approximately 20 h, which allowed the reaction to go to completion. The solvent was then removed, and the product, Cu(hfac)$_2$·H$_2$O, was dried under vacuum: IR (KBr) 3564 (br) ν(H$_2$O), 1643 (s) ν(C···O), 1611 (m) ν(C···C), 1562 (s) ν(C···O) + δ(CH), 1534 (m), 1474 (s), 1359 (w) ν(C···C) + ν(CF$_3$), 1256 (vs) ν(CF$_3$), 1218 (s), 1147 (vs) β(CH), 1109 (m), 810(s) γ(CH) + ν(C−CF$_3$), 750 (m) ν(C−CF$_3$), 679 (s), 597 (s), 526 (m).

The above reaction was also conducted in scCO$_2$: Cu$_2$(O$_2$CCH$_3$)$_4$·2H$_2$O (**3**) (1.2×10^{-4} mol), contained in a glass holder, and hfacH (2.9×10^{-4} mol) were placed in a sapphire-windowed 2.5-mL high-pressure view cell. The cell was then charged with scCO$_2$ (214 ± 3 bar, 40 ± 2 °C). A green solution, indicative of Cu(hfac)$_2$·H$_2$O, resulted immediately. The reaction, which was monitored by UV−visible spectroscopy, went to completion in less than 1 min: UV−visible λ_{max} 675 nm.

Table 1. Crystallographic Data for **1** and **2**

	1	**2**
formula	C$_{12}$H$_8$F$_{12}$O$_7$Cu	C$_{12}$H$_8$F$_{12}$O$_7$Zn
mol wt (g/mol)	555.72	557.57
cryst color	green	white
cryst system	monoclinic	orthorhombic
space group	$P2_1/n$ (No. 14)	*Cmca* (No. 64)
cryst dimens (mm)	$0.30 \times 0.25 \times 0.15$	$0.35 \times 0.10 \times 0.10$
a (Å)	13.8024(6)	21.4274(24)
b (Å)	20.8587(8)	7.4996(8)
c (Å)	14.2894(5)	23.8542(25)
α (deg)	90	90
β (deg)	114.76	90
γ (deg)	90	90
V (Å^3)	3735.8(3)	3833.3(7)
Z	8	8
ρ_{calc} (g/cm^3)	1.976	1.922
μ (mm^{-1})	1.321	1.43
rflcns collcd	26 246	35 112
rflcns (unique)	9035	1752
R (all data)[a]	0.1032	0.085
R_w (all data)[b]	0.2024	0.128
GOF[c]	1.044	3.4731

[a] $R = \Sigma||F_o| - |F_c||/\Sigma|F_o|$. [b] $R_w = [\Sigma(w(|F_o| - |F_c|)^2)/\Sigma(w|F_o|)^2)]^{1/2}$. [c] GOF $= [\Sigma(w(|F_o| - |F_c|)^2)/(\text{no. of reflections} - \text{no. of parameters})]^{1/2}$.

X-ray Structure Determinations. X-ray crystallographic data for **1** and **2** were collected at −100 °C on a Bruker SMART 1K CCD diffractometer with Mo Kα radiation ($\lambda = 0.710\ 73$ Å), using the ω-scan mode. The structures were solved by direct methods and refined by a full-matrix least-squares method. Calculations for **1** were performed using the Bruker SHELXTL program package,[14] and computations for **2** were performed using the NRCVAX suite of programs.[15] Analysis of the results of **1** with MISSYM indicated the presence of noncrystallographic translational symmetry. Close examination of intensity data from several samples indicated that the doubled unit cell was indeed the correct one. The pseudosymmetry gave rise to higher than normal correlation factors in the final refinement steps. Details of the crystal data and intensity collections for **1** and **2** are summarized in Table 1, while selected bond lengths and angles are tabulated in Tables 3 for **1** and 4 for **2**. Complete tables of bond lengths and angles are given in Tables S1−S3 (Supporting Information).

Blank NMR Studies. All experiments were performed at 40 °C under nitrogen. A copper or zinc coupon (1 equiv) combined with only *t*-BuPA (0.1 equiv) in CD$_2$Cl$_2$ resulted in no peroxy ester decomposition within 24 h as observed by NMR spectroscopy.

(14) *SHELXTL PC*, version 4.2/360; Bruker Analytical X-ray Instruments, Inc.: Madison, WI, 1994.
(15) Gabe, E. J.; Le Page, Y.; Charland, J. P.; Lee, F. L.; White, P. S. *J. Appl. Crystallogr.* **1989**, *22*, 384.

Table 2. Reaction of Cu(0) and *t*-BuPA (or EPDC) with a Series of β-Diketone Ligands

		t-BuPA oxidant			
ligand	ligand pK_{a1}[19,a]	Cu(0) removed (%)	monolayers of Cu(0) removed	avg dissolution rate (nm/min)	EPDC oxidant avg dissolution rate (nm/min)
hfacH	6.0	14	6.9×10^4	3.9	10.7
tmhdH	15.9	4	2.0×10^4	1.1	3.9
tfacH	8.8	1	5.7×10^3	0.3	3.3

[a] pK_a values measured in dioxane (75%)−water mixture at 30 °C.

In a second blank experiment, a stirred solution of *t*-BuPA (1 equiv) and hfacH (3 equiv) in CD_2Cl_2 (or hexane-d_{14}) was monitored by ^{1}H NMR spectroscopy. The originally colorless solution turned bright orange ($\lambda_{max} = 388$ and 446 nm) over time, suggesting a conjugated system. The hfacH O*H* proton shifted from approximately 12.29 ppm ($t = 0$ min) to 11.00 ppm ($t = 35$ h). ^{1}H and ^{19}F NMR spectroscopies indicated that the hfacH (98% at $t =$ 0 min) slightly hydrolyzed to 1,1,1,5,5,5-hexafluoro-4,4-dihydroxy-2-pentanone (2%) and 1,1,1,5,5,5-hexafluoro-2,2,4,4-pentanetetrol (9%) within 35 h.[16] No resonances for peroxy ester decomposition products were observed.

Copper Metal with *t*-BuPA and hfacH NMR Studies. A solution of *t*-BuPA (0.03 mL, 2×10^{-4} mol) and hfacH (0.07 mL, 5×10^{-4} mol) was stirred in 2 mL of CD_2Cl_2 (or hexane-d_{14}) at 40 °C under nitrogen. The copper coupon (0.095, 1.5×10^{-3} mol) was then added to the colorless solution. An aliquot was immediately transferred to the NMR spectrometer, and the ^{1}H NMR spectrum was acquired at room temperature ($t = 0$ min). This aliquot was immediately returned to the reaction mixture. The copper reaction was monitored every 5 h for 33.5 h.

Zinc Metal with *t*-BuPA and hfacH NMR Studies. A zinc coupon was treated with *t*-BuPA and hfacH in CD_2Cl_2 at 40 °C under nitrogen. The same procedure and amounts of reagents were used as described above for copper. The zinc reaction was monitored every 20 min for 280 min. The peroxy ester completely decomposed after 220 min. This reaction mixture was then stirred for approximately 3 d, and the white solid was collected by filtration, washed with hexanes and pentane, and dried under vacuum. Product **2** and Zn(hfac)$_2$·2H$_2$O were confirmed by ^{1}H NMR spectroscopy.

An analogous reaction was performed using a 10-mL high-pressure view cell with $scCO_2$ (40 °C, 214 bar) as the solvent. The *t*-BuPA (0.45 mL, 2.3×10^{-3} mol), hfacH (0.53 mL, 3.8×10^{-3} mol), and a zinc coupon (0.098 g, 1.5×10^{-3} mol, contained in a glass holder) were placed in the cell. The cell was charged with CO_2 (214 ± 3 bar, 40 ± 2 °C). The originally colorless solution resulted in a pale yellow, homogeneous solution (except for the zinc coupon) within 5 h. After 6 d of stirring, the cell was vented into a vial containing CD_2Cl_2, and the ^{1}H NMR spectrum was immediately taken, confirming the presence of unreacted *t*-BuPA, *tert*-butyl alcohol, and acetic acid. Analysis of the NMR spectrum showed 31% (7.0×10^{-4} mol) of *t*-BuPA and 36% (1.4×10^{-3} mol) of hfacH were consumed. These percentages were calculated from the integral areas of *t*-BuPA, *tert*-butyl alcohol, and hfacH normalized to the total amount of *t*-BuPA and hfacH initially added. The remaining zinc coupon was washed with MeOH and acetone, dried, and weighed. Approximately 46% of Zn(0) (6.9×10^{-4} mol) dissolved in the *t*-BuPA/hfacH etchant solution. These data confirm the 1:1:2 (Zn:*t*-BuPA:hfacH) stoichiometry of the reaction.

***t*-BuPA Decomposition by Zinc.** A zinc coupon (0.098 g, 1.5×10^{-3} mol) was treated with *t*-BuPA (0.45 mL, 2.3×10^{-3} mol) in 10 mL of hexanes at 40 °C under argon. This mixture was gently stirred for 19 h. The coupon was thoroughly washed with hexanes, air-dried, and transferred into a flask containing hfacH (0.05 mL) and CD_2Cl_2. This mixture was stirred at room temperature for 1 h. The ^{1}H NMR spectrum of a solution aliquot showed *tert*-butyl alcohol, acetone, and acetic acid in a ratio of 1:2:3. When an analogous reaction was conducted in a glovebox, acetone was still observed as a decomposition product.

Results and Discussion

Dissolution of Copper Metal in $scCO_2$. Copper coupons were treated with the oxidant, *t*-BuPA, and a β-diketone chelating agent in $scCO_2$ (40 °C, 214 bar) for 20 h. The originally colorless *t*-BuPA/β-diketone solution in $scCO_2$ transforms to a green, homogeneous solution after only a few minutes. The reaction was allowed to proceed for 20 h to obtain accurate Cu(0) weight differences.

Table 2 shows the effect of ligand variations on copper removal. Copper removal increases in the order tfacH < tmhdH < hfacH. A similar trend in copper removal is observed when EPDC is used as the oxidant;[6] however, the average dissolution rate is significantly greater in the EPDC reactions (Table 2). This rate difference is attributed to the higher reactivity of EPDC ($t_{1/2} = 28$ h at 40 °C) compared to *t*-BuPA ($t_{1/2} = 145$ h at 40 °C).[17,18] Although hfacH is the poorest ligand among those investigated, it is the strongest acid due to the presence of two electron-withdrawing CF_3 groups[19] and yields the most soluble copper complex in CO_2.[20,21] The role that the ligand properties and the solubility of the resulting metal complexes play in the reaction is discussed below (working model of the oxidative dissolution reaction). Due to its high reactivity, hfacH was employed for all subsequent studies.

Metallic Copper Oxidation and Chelation with *t*-BuPA and hfacH: Synthesis and Characterization of Resulting Copper Complex. In preparative scale reactions, copper powder is used as the metal source instead of a copper coupon to reduce the overall reaction time and to allow the reactions to go to completion. Treatment of copper powder with *t*-BuPA and hfacH at 40 °C in hexanes affords a homogeneous green solution. Green crystals of *trans*-Cu(hfac)$_2$(H$_2$O)(CH$_3$CO$_2$H) (**1**) (Scheme 1) are obtained from slow evaporation of the original reaction mixture. The water

(16) Aygen, S.; Van Eldik, R. *Chem. Ber.* **1989**, *122*, 315.
(17) Brandrup, J.; Immergut, E. H. *Polymer Handbook*, 3rd ed.; Wiley & Sons: New York, 1989.
(18) The half-life of *t*-BuPA at 40 °C was determined by extrapolation of the following data: $t_{1/2} = 13$ h at 100 °C, 2 h at 115 °C, and 0.3 h at 130 °C.
(19) Yokoi, H.; Kishi, T. *Chem. Lett.* **1973**, *7*, 749.
(20) Lagalante, A. F.; Hansen, B. N.; Bruno, T. J.; Sievers, R. E. *Inorg. Chem.* **1995**, *34*, 5781.
(21) Lin, Y.; Wai, C. M. *Anal. Chem.* **1994**, *66*, 1971.

Scheme 1. Reaction of M(0) with *t*-BuPA and HfacH (M = Cu; M = Zn; Y = H_2O)

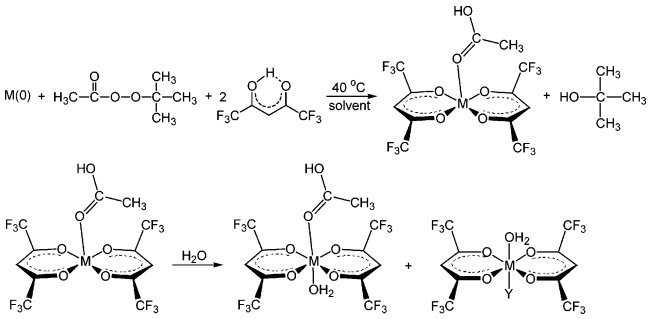

Table 3. Selected Bond Lengths (Å) and Angles (deg) for **1**

Cu1−O23	1.948(3)	C20−C21	1.390(5)
Cu1−O6	1.953(3)	C21−C22	1.391(6)
Cu1−O10	1.957(3)	C7−C11	1.541(6)
Cu1−O19	1.962(3)	C9−C15	1.548(6)
Cu1−O1	2.318(4)	C20−C24	1.535(6)
Cu1−O2	2.382(4)	C22−C28	1.539(6)
O2−C3	1.201(6)	C9−O10	1.268(5)
C3−O4	1.331(6)	C7−O6	1.242(5)
C3−C5	1.488(6)	C22−O23	1.268(5)
C7−C8	1.393(6)	C20−O19	1.254(4)
C8−C9	1.365(6)		
O10−Cu1−O19	175.9(1)	O10−Cu1−O1	90.5(1)
O1−Cu1−O2	177.1(1)	O10−Cu1−O2	91.3(1)
O23−Cu1−O6	179.0(1)	O6−Cu1−O10	92.5(1)
O6−Cu1−O2	83.2(1)	O23−Cu1−O19	92.6(1)
O19−Cu1−O2	84.7(1)	O19−Cu1−O1	93.5(1)
O23−Cu1−O1	86.3(1)	O6−Cu1−O1	94.4(1)
O23−Cu1−O10	86.8(1)	O2−Cu1−O23	96.1(1)
O6−Cu1−O19	88.0(1)	C3−O2−Cu1	133.1(3)

ligand arises either from adventitious water in the solvent or from protonation of the initial copper oxide layer with hfacH. The product formulation of **1** was established by a single-crystal X-ray structure determination.

An ORTEP diagram of **1** is depicted in Figure 1. Complex **1** crystallizes with two crystallographically independent isostructural molecules in the asymmetric unit. Metric data are presented for one of the molecules. The coordination environment around Cu1 is pseudooctahedral with the water and acetic acid ligands occupying trans positions (Table 3). The metal−ligand bond distances and angles correspond well with those in the *trans*-[Cu(hfac)$_2$(H$_2$O)$_2$]·H$_2$O complex.[22] The Cu1−O(hfac$^-$) bond distances average 1.955(6) Å, while the Cu1−O1(water, 2.318(4) Å) and Cu1−O2(acetic acid, 2.382(4) Å) distances are significantly elongated due to a Jahn−Teller distortion. The carbonyl group of the acetic acid ligand is coordinated to copper, as indicated by the bond distances for the acetic acid moiety (C3−O2 = 1.201(6) Å and C3−O4 = 1.331(6) Å). The C=O distance in **1** is similar to the reported C=O distances in uncoordinated acetic acid (1.24(2) Å)[23] and in [Ni(CH$_3$CO$_2$H)$_6$][BF$_4$]$_2$ (1.217(5) Å).[24] An extensive hydrogen-bonding network is present in the solid-state structure of **1**. The acetic acid hydroxyl H and O atoms (H4 and O4), the hfac$^-$ O atoms (O19 and O6), and

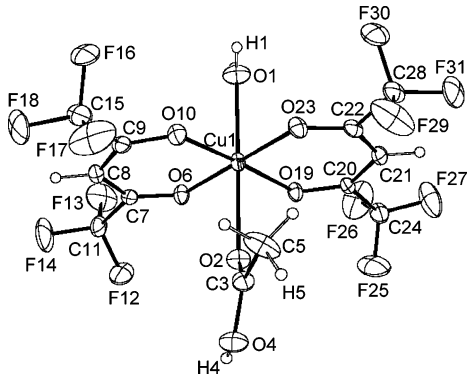

Figure 1. ORTEP diagram of **1** with thermal ellipsoids drawn at the 50% probability level. Only one of the two crystallographically independent molecules is shown.

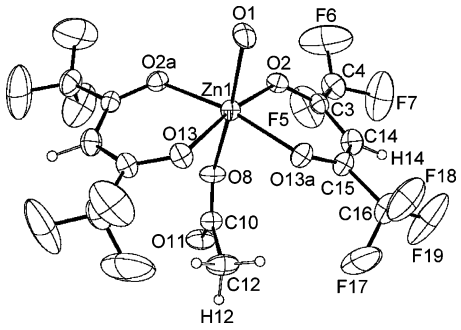

Figure 2. ORTEP diagram of **2** with thermal ellipsoids drawn at the 50% probability level.

one of the water hydrogen atoms (H1) are hydrogen-bonded to four neighboring complexes.

The solid-state IR spectrum of **1** has the expected bands for the coordinated aqua and hfac$^-$ ligand on the basis of the data for Cu(hfac)$_2$·H$_2$O.[25] A sharp band is observed at 1718 cm^{-1}, which is assigned to the C=O stretch for the acetic acid ligand. This band is shifted 63 cm^{-1} to lower energy from the ν(C=O) stretch in uncoordinated acetic acid (1781 cm^{-1}),[26−28] indicative of metal coordination.[27] The CH_2Cl_2 solution IR spectrum of **1** shows two C=O stretches at 1718 and 1764 cm^{-1}, which are assigned to coordinated and uncoordinated acetic acid, respectively, indicating that the acetic acid ligand partially dissociates in CH_2Cl_2 solution.

Metallic Zinc Oxidation and Chelation with *t*-BuPA and hfacH: Synthesis and Characterization of Resulting Zinc Complexes. The analogous zinc reaction proceeds much more rapidly than the copper reaction. The zinc coupon completely dissolved within 2 h after treatment with *t*-BuPA and hfacH in hexanes (Scheme 1), resulting in a homogeneous pale yellow solution. X-ray-quality white crystals of *trans*-Zn(hfac)$_2$(H$_2$O)(CH$_3$CO$_2$H) (**2**) precipitate upon cooling the original reaction mixture.

An ORTEP view of **2** is given in Figure 2. The zinc complex **2** adopts a pseudooctahedral geometry similar to

(22) Maverick, A. W.; Fronczek, F. R.; Maverick, E. F.; Billodeaux, D. R.; Cygan, Z. T.; Isovitsch, R. A. *Inorg. Chem.* **2002**, *41*, 6488.
(23) Jones, R. E.; Templeton, D. H. *Acta Crystallogr.* **1958**, *11*, 484.
(24) Cramer, R. E.; Van Doorne, W.; Dubois, R. *Inorg. Chem.* **1975**, *14*, 2462.
(25) Morris, M. L.; Moshier, R. W.; Sievers, R. E. *Inorg. Chem.* **1963**, *2*, 411.
(26) *The Aldrich Library of FT-IR Spectra*, 1st ed.; Pouchert, C. J., Ed.; Aldrich Chemical Co.: Milwaukee, WI, 1985.
(27) Patten, K. O., Jr.; Andrews, L. *J. Phys. Chem.* **1986**, *90*, 1073.
(28) Hasan, M. A.; Zaki, M. I.; Pasupulety, L. *Appl. Catal., A* **2003**, *243*, 81.

Table 4. Selected Bond Lengths (Å) and Angles (deg) for **2**

Zn1−O1	2.06(1)	C3−C14	1.38(1)
Zn1−O2	2.06(1)	C15−C14	1.39(1)
Zn1−O13	2.06(1)	C3−C4	1.52(1)
Zn1−O8	2.34(1)	C15−C16	1.53(1)
O8−C10	1.20(1)	C3−O2	1.25(1)
C10−O11	1.30(1)	C15−O13	1.25(1)
C10−C12	1.51(1)		
O1−Zn1−O8	168.3(3)	O8−Zn1−O13	92.2(1)
O2−Zn1−O13	169.8(1)	O1−Zn1−O2	93.1(1)
O2−Zn1−O8	79.2(1)	O1−Zn1−O13	96.2(1)
O13−Zn1−O13a	87.4(1)	O2−Zn1−O2a	96.3(1)
O2−Zn1−O13a	87.4(1)	Zn1−O8−C10	138.4(6)

the copper complex **1**. A crystallographic mirror plane containing Zn1 and the trans acetic acid and aqua ligands bisects the molecule. The $hfac^-$ ligands are domed out of the equatorial plane toward the acetic acid ligand (Table 4). The Zn1−O($hfac^-$) (2.06(1) Å) and Zn1−O1(water) (2.06(1) Å) bond distances are similar to each other and are significantly shorter than Zn1−O8(acetic acid, 2.34(1) Å). The carbonyl group of the acetic acid is coordinated to zinc like for **1**, as indicated by the metric parameters of the acetic acid ligand (C10−O11 = 1.30(1) Å; O8−C10 = 1.20(1) Å). The Zn−ligand bond distances correspond well with the *trans*-Zn(hfac)$_2$·2H$_2$O[29] and Zn(hfac)$_2$·2H$_2$O·diglyme[30] complexes. The average Zn1−O($hfac^-$) bond distance in **2** is nearly 0.11 Å longer than for the copper complex, while the M−O(water) and M−O(acetic acid) are both shorter in **2** than in **1** (by 0.26 and 0.04 Å, respectively). An extensive hydrogen-bonding network is also present in the solid-state structure of **2**. The water hydrogen atoms, the $hfac^-$ O atoms (O13 and O13a), and the acetic acid hydroxyl H and carbonyl O atoms are hydrogen-bonded to three adjacent complexes.

The isolated zinc product is contaminated with Zn(hfac)$_2$·2H$_2$O, and elemental analysis of the solid fits to a 1:1 mixture of **2** and Zn(hfac)$_2$·2H$_2$O. Solid **2** (+Zn(hfac)$_2$·2H$_2$O) was characterized by ^{1}H and ^{13}C NMR spectroscopy in acetone-d_6. The ^{1}H NMR spectrum of **2** (+Zn(hfac)$_2$·2H$_2$O) shows two singlets at δ 5.93 and 1.95 ppm, corresponding to the protons from $hfac^-$ and the methyl group of the acetic acid, respectively. A ^{1}H−^{13}C COSY NMR spectrum confirms that the resonance at 1.95 ppm corresponds to the methyl protons and not the water protons (Figure S1). The integrated ratio of acetic acid (CH_3):hfac (C−H) of 3:4 is consistent with the elemental analysis results. No resonances are observed for the coordinated water molecule or the acidic proton of acetic acid, presumably due to chemical exchange.[31] It should be noted that acetone is expected to be a better ligand than acetic acid and would likely displace acetic acid from the coordination sphere of zinc. The ^{13}C{^{1}H} NMR spectrum (Figure S2) shows resonances for acetic acid and the coordinated $hfac^-$.

The solid-state IR spectrum of **2** (+Zn(hfac)$_2$·2H$_2$O) has the expected bands for the coordinated aqua and $hfac^-$ ligands on the basis of the data for Zn(hfac)$_2$·2H$_2$O.[25] A band at 1733 cm^{-1} is observed for ν(C=O) of the coordinated acetic acid ligand. This stretch is 15 cm^{-1} higher in energy than the corresponding stretch for **1**.

Spectroscopic Investigation of the Decomposition Products of *t*-BuPA on Reaction with Metallic Copper or Zinc and hfacH. The metallic zinc reaction appears to proceed similarly to the copper reaction on the basis of the structures of the oxidized metal complexes, **1** and **2**. NMR spectroscopy was used as a tool to monitor the peroxy ester decomposition reaction. In control reactions of *t*-BuPA and hfacH in CD_2Cl_2 (or hexane-d_{14}) at 40 °C, no resonances are observed for peroxy ester decomposition products after 35 h, indicating that the hfacH alone does not promote *t*-BuPA decomposition. Further, in reactions of copper or zinc metal with only *t*-BuPA in CD_2Cl_2 at 40 °C, no resonances are observed for peroxy ester decomposition products after 24 h, confirming the requirement of both hfacH and *t*-BuPA to carry out the oxidative dissolution reaction.

In the NMR experiments to study the oxidative dissolution reactions, an excess of metal reagent is employed to enhance the reaction rate. For the copper reaction in CD_2Cl_2 at 40 °C, as the reaction proceeds, dissolution of paramagnetic Cu(hfac)$_2$ results in a severe broadening and shifting of the resonances for *t*-BuPA and the decomposition products, limiting the utility of NMR spectroscopy. An experiment conducted in hexanes-d_{14} shows the same reaction products resonances, indicating that the reaction products are independent of the solvent chosen here.

Time-dependent ^{1}H NMR spectra for the zinc reaction in CD_2Cl_2 are more informative (Figure 3). Signals A and B are assigned to the *tert*-butyl and methyl hydrogens of *t*-BuPA, respectively. After 20 min, product signals C−E appear in the spectrum, and the reaction is complete at 220 min. The product chemical shifts are assigned to *tert*-butyl alcohol (C, HOC(CH_3)$_3$; D, *H*OC(CH_3)$_3$,) and acetic acid (E, C*H*$_3$). Equimolar amounts of *tert*-butyl alcohol and acetic acid are formed, as illustrated by the normalized integrations (Figure 4). The Zn(hfac)$_2$ product precipitates from solution as a white solid as the reaction proceeds, and therefore, no resonances are observed for the zinc product. Since acetic acid appears in the correct molar ratio in the supernatant, the solid that precipitates from CD_2Cl_2 must not have acetic acid coordinated. The expected resonances are observed in the ^{13}C NMR spectrum of the reaction mixture (Figure S3), and assignments are made on the basis of the ^{1}H−^{13}C COSY NMR spectrum (Figure S4). Only one resonance is observed in the ^{19}F NMR spectrum of this solution at $t \geq 220$ min, implying that the enolate ion did not decompose.

To confirm that the *t*-BuPA products are identical for reactions conducted in $scCO_2$, the reaction of zinc with the etchant solution was conducted in $scCO_2$. After reacting for 6 days, the remaining zinc coupon was washed and weighed, and an ^{1}H NMR (CD_2Cl_2) of the reaction mixture was taken to evaluate the extent of the reaction on the basis of the amount of zinc consumed. Signals were observed for unreacted *t*-BuPA, its decomposition products (*tert*-butyl alcohol and acetic acid), and free hfacH (Figure S5). The

(29) Adams, R. P.; Allen, H. C., Jr.; Rychlewska, U.; Hodgson, D. J. *Inorg. Chim. Acta* **1986**, *119*, 67.
(30) Gulino, A.; Castelli, F.; Dapporto, P.; Rossi, P.; Fragalà, I. *Chem. Mater.* **2000**, *12*, 548.
(31) Chattoraj, S. C.; Cupka, A. G., Jr.; Sievers, R. E. *J. Inorg. Nucl. Chem.* **1966**, *28*, 1937.

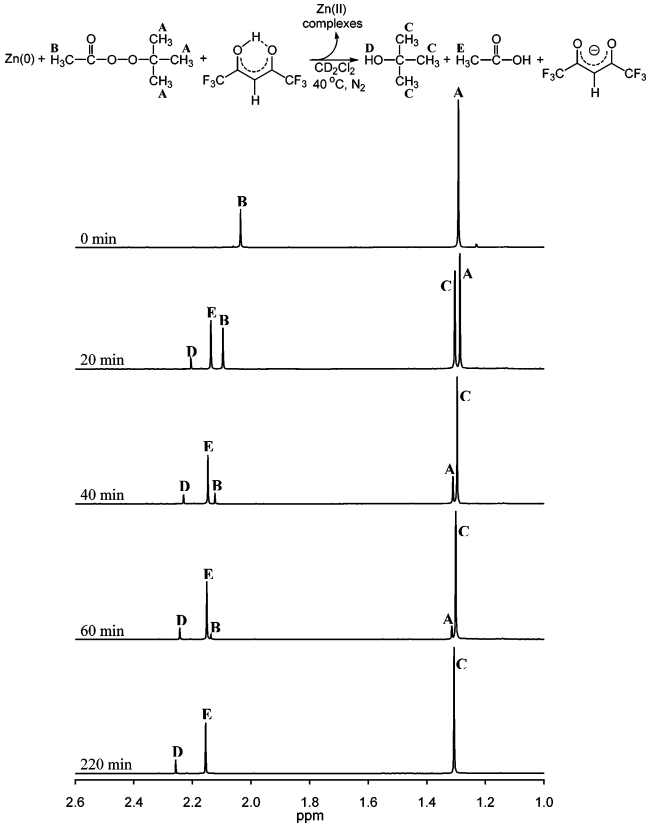

Figure 3. Selected time-dependent ^{1}H NMR spectra during the reaction of zinc metal (1 equiv) with *t*-BuPA (0.10 equiv) and hfacH (0.33 equiv) in CD_2Cl_2. Benzene was used as the calibration standard. The hfacH signals are not shown.

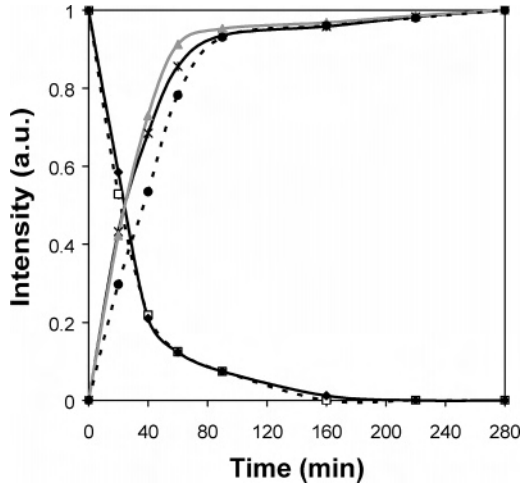

Figure 4. Plot of integral areas normalized to one hydrogen for *t*-BuPA ((◆) C(C*H*$_3$)$_3$; (□) C*H*$_3$)), *tert*-butyl alcohol ((△) C(C*H*$_3$)$_3$; (●) O*H*), and acetic acid ((*) C*H*$_3$) over time for the reaction of zinc metal (1 equiv) with *t*-BuPA (0.10 equiv) and hfacH (0.33 equiv) in CD_2Cl_2 at 40 °C.

reaction stoichiometry was confirmed as 1:1:2 (Zn:*t*-BuPA:hfacH), demonstrating that *t*-BuPA acts as an overall two electron oxidant for zinc.

Solvent Effects. The reactions of copper and zinc metal with the etchant solution yield a similar product distribution in $scCO_2$, hexanes, and CD_2Cl_2. For the hexanes and $scCO_2$ reactions of metallic zinc with *t*-BuPA and hfacH, the same reagent concentrations were used, so the results can be directly compared. When hexanes is used as the reaction medium, the zinc coupon completely dissolves within 2 h; however, when $scCO_2$ is used as the solvent, only 46% of the zinc coupon dissolves after 6 days of reaction, indicating that the overall reaction rate is significantly slower in $scCO_2$ than hexanes. These solvents differ in polarities, dielectric constants, and densities (Table 5),[32] but the origin of the rate differences with solvent for this reaction is not understood in detail.

Table 5. Comparison of the Solvent Polarities, Dielectric Constants, and Densities[32]

solvent	dipole moment (D)	dielectric constant	density (g/mL)
CO_2	0	1.52[a]	0.852[b]
hexane	0	1.89 (20 °C)	0.656 (25 °C)
methylene chloride	1.60	9.08 (20 °C)	1.31 (25 °C)

[a] Value refers to $scCO_2$ (40 °C, 215 bar).[47] [b] Value refers to $scCO_2$ (40 °C, 214 bar).[48]

Oxidation of Metallic Copper or Zinc with *t*-BuPA. The observation of a blue solution upon EtOH washing of copper powder treated with *t*-BuPA in hexanes prompted additional experiments to identify the reaction products in the absence of added hfacH. Reaction between copper powder and a hexanes solution of *t*-BuPA in EtOH at 40 °C yields a blue solution. A blue solid was isolated after removal of solvent, which was identified as the well-known dicopper(II) tetraacetate dihydrate complex, $Cu_2(O_2CCH_3)_4{\cdot}2H_2O$, by a single-crystal X-ray determination,[33,34] IR spectroscopy,[35] and elemental analysis. Quantification of the amount of copper consumed relative to **3** produced shows that all of the copper dissolved ends up as **3** within experimental error. This result combined with the fact that 4 equiv of acetate is available to form **3** implies that the *t*-BuPA acts as a one-electron oxidant for copper in EtOH solution (eq 3). The *t*-BuO$^\bullet$ product, which is required for a balanced reaction, apparently does not play a role in oxidation of copper in EtOH solvent. Solid **3** reacts immediately with hfacH in hexanes or $scCO_2$ to form $Cu(hfac)_2{\cdot}H_2O$(soln) and acetic acid (eq 4), suggesting that the exchange of coordinated acetate for hfac$^-$ would be favorable under the etching reaction conditions.

$$\mathrm{Cu(s) + 2}t\text{-BuO}-\mathrm{OAc + H_2O} \xrightarrow{\mathrm{EtOH}} \underset{\mathbf{3}}{{}^1/_2\mathrm{Cu_2(O_2CCH_3)_4{\cdot}2H_2O(soln)}} + 2t\text{-BuO}^\bullet \quad (3)$$

$$\underset{\mathbf{3}}{{}^1/_2\mathrm{Cu_2(O_2CCH_3)_4{\cdot}2H_2O(s)}} + \mathrm{2hfacH} \rightarrow \mathrm{Cu(hfac)_2{\cdot}H_2O(soln) + 2CH_3CO_2H} \quad (4)$$

As mentioned above, no soluble products are observed by NMR spectroscopy upon reaction of *t*-BuPA with copper and zinc metal in CD_2Cl_2 solution. To determine if there are *t*-BuPA decomposition products associated with the metal surface in hexanes, a two-step reaction was conducted for

(32) *CRC Handbook of Chemistry and Physics*, 74th ed.; Lide, D. R., Ed.; CRC Press: Boca Raton, FL, 1993.
(33) Van Niekerk, J. N.; Schoening, F. R. L. *Acta Crystallogr.* **1953**, *6*, 227.
(34) Brown, G. M.; Chidambaram, R. *Acta Crystallogr., Sect. B* **1973**, *29*, 2393.
(35) Mathey, Y.; Greig, D. R.; Shriver, D. F. *Inorg. Chem.* **1982**, *21*, 3409.

zinc to enable NMR spectroscopy to be used as a characterization tool. A zinc coupon was first treated with *t*-BuPA in hexanes, thoroughly washed with hexanes, air-dried, and then transferred to an hfacH/CD_2Cl_2 solution and stirred for 1 h. ^{1}H NMR spectroscopy of a solution aliquot showed *tert*-butyl alcohol, acetone, and acetic acid in a 1:2:3 molar ratio. An experiment performed in a glovebox, avoiding exposure to air, also showed acetone as a decomposition product. It is proposed that both acetone and *tert*-butyl alcohol are produced from a surface-bound *t*-BuO species. This proposal is supported by the fact that the sum of the amounts of *tert*-butyl alcohol and acetone observed is equal to the amount of acetic acid. The initial oxide coating on the surface present in this experiment would provide different reaction sites to the *t*-BuO• radical than in the one-pot reaction and may explain why different products are observed in the two-step reaction. Acetone most likely arises from β-scission of *t*-BuO• radical, which is presumably released from the surface upon reaction with hfacH.[36−39] This experiment provides evidence that even though no soluble products are formed upon reaction of zinc with *t*-BuPA, *t*-BuPA does react with the zinc surface in the absence of added hfacH and that hfacH plays a role in removing the *t*-BuPA reaction products from the surface.

Working Model for the Oxidative Dissolution Reaction. On the basis of the above experiments, several features emerge that are relevant to the mechanism of the CMP reaction, which are discussed below.

(1) Reductive Cleavage of Peroxy Esters. The peroxy ester, *t*-BuPA, is thermally stable, with a half-life of 13 h at 100 °C.[17] Accordingly, thermal decomposition of *t*-BuPA is not expected to be an important reaction pathway under the conditions of our oxidative dissolution reactions. In addition, NMR experiments establish that the decomposition of *t*-BuPA is not promoted by hfacH, the other reagent in the reaction. Therefore, it is most likely that the decomposition of *t*-BuPA is initiated by the metal(0) source acting as a reducing agent for *t*-BuPA. There is precedence for reductive initiation of the decomposition of peroxy esters. Cu(I) salts are homogeneous catalysts for the decomposition of peroxy esters.[39] These reactions proceed by a one-electron transfer from Cu(I) to the peroxy ester, yielding Cu(II), acetate, and *t*-BuO$^\bullet$. A reductive cleavage mode of reaction for peroxy esters is also supported by recent electrochemical studies.[40] The electrochemical data in DMF solution for *t*-BuOOC(O)*t*-Bu are consistent with a concerted electron transfer/O−O bond cleavage reaction to yield acetate and *t*-BuO$^\bullet$ (eq 5). The *t*-BuO$^\bullet$ is reduced in a step after the cleavage reaction (eq 6).

$$t\text{-BuOOC(O)}t\text{-Bu} + e^- \rightarrow t\text{-BuCO}_2^- + t\text{-BuO}^\bullet \quad (5)$$

$$t\text{-BuO}^\bullet + e^- \rightarrow t\text{-BuO}^- \quad (6)$$

For the two metal reducing agents employed in this study, on the basis of the aqueous reduction potentials, zinc provides nearly 1 V more driving force for the reduction reaction than copper,[41] consistent with the more rapid reaction of zinc. In nonpolar $scCO_2$ or hexanes media, the anionic reduction products would be associated with the metal surface.

(2) Stoichiometry of the Oxidation Reaction and Working Model. In the reaction of zinc with the *t*-BuPA/hfacH etchant solution, NMR studies establish that *t*-BuPA cleanly decomposes to *tert*-butyl alcohol and acetic acid under an inert atmosphere. The product distribution after partial etching of zinc confirms that *t*-BuPA acts as an overall two-electron oxidant for Zn(0) in $scCO_2$ solvent.

A possible working model for the oxidative dissolution of copper or zinc metal by reaction with the *t*-BuPA/hfacH etchant solution that takes into account these features and the known mode of reaction of *t*-BuPA is given in eqs 7 and 8. At the outset of the reaction, the metal coupons will have a surface layer of oxide,[1,6] which passivates the surface. Given that the etching reaction proceeds without a pretreatment to remove the oxide surface, it is likely that hfacH is effective in removing this passivating layer under the reaction conditions. The scheme begins with an unpassivated metal surface, written as M_n(s). In hexanes and CO_2 media, we propose that the *t*-BuPA is reduced at the surface of the metal to form acetate and *t*-butoxide bound to the metal surface (eq 7). The very low dielectric constants of the hexanes and $scCO_2$ media (Table 5) dictate that these redox reactions must occur at the surface of the metal. The proposal that the *t*-BuPA cleavage products associate with the metal surface is supported by the fact that (1) the reaction of copper or zinc with *t*-BuPA in the absence of added hfacH is very limited and no peroxy ester decomposition products are observed in solution by NMR spectroscopy, (2) pretreatment of a Zn(0) coupon with *t*-BuPA followed by reaction with hfacH shows soluble products derived from *t*-BuPA cleavage, and (3) EtOH washing of a Cu(0) coupon treated with *t*-BuPA in hexanes yields soluble $Cu_2(O_2CCH_3)_4 \cdot 2H_2O$.

$$M_n(s) + t\text{-BuOOAc} \rightarrow M_n^{2+}(OAc)^-(O\text{-}t\text{-Bu})^-(s) \quad (7)$$

$$M_n^{2+}(OAc)^-(O\text{-}t\text{-Bu})^-(s) + 2\text{hfacH} \rightarrow M_{n-1}(s) + M(\text{hfac})_2(\text{soln}) + \text{AcOH} + t\text{-BuOH} \quad (8)$$

For the metal coupon reactions, metal dissolution requires both *t*-BuPA and hfacH. In addition to removing the initial oxide layer, hfacH has a critical second role in protonating the surface-bound acetate and *t*-butoxide ligands to produce acetic acid and *tert*-butyl alcohol (eq 8), thereby facilitating their desorption from the surface. The pK_a of the β-diketone and the coordinating ability of the conjugate ion will dictate the thermodynamic driving force for the removal of the surface bound species. While we have not experimentally observed surface bound M(hfac) intermediates, on the basis of gas-phase studies,[7−11,42−46] it is reasonable to propose that

(36) Walling, C.; Zavitsas, A. A. *J. Am. Chem. Soc.* **1963**, *85*, 2084.
(37) Colombani, D.; Maillard, B. *J. Chem. Soc., Perkin Trans. 2* **1994**, *4*, 745.
(38) Kochi, J. K. *J. Am. Chem. Soc.* **1962**, *84*, 774.
(39) Kochi, J. K.; Mains, H. E. *J. Org. Chem.* **1965**, *30*, 1862.
(40) Antonello, S.; Formaggio, F.; Moretto, A.; Toniolo, C.; Maran, F. *J. Am. Chem. Soc.* **2001**, *123*, 9577.
(41) Silberberg, M. *Chemistry: The Molecular Nature of Matter and Change*; Mosby: St. Louis, MO, 1996.

eq 8 proceeds via exchange of the surface-bound M(OAc) and M(O-*t*-Bu) species to produce surface-bound M(hfac). To ultimately extract a M(II) ion from the surface, it is necessary for two $hfac^-$ ligands to coordinate to a single M(II) ion and for the $M(hfac)_2$ complex, produced at the metal surface, to dissolve into solution.

The ability to remove the $M(hfac)_2$ product from the metal surface into solution could influence the rate of metal dissolution. The etching ability of the various chelating ligands toward copper metal in $scCO_2$ (Table 2) correlates well with the solubility of the copper(II) complexes in $scCO_2$ [we have chosen to compare similar reaction conditions, i.e., $P = 207$ bar, $T = 40$ °C, $d = 0.847$ g/mL, and mole fraction solubilities $Cu(tfac)_2$ (4.2×10^{-4}), $Cu(tmhd)_2$ (5.8×10^{-4}), and $Cu(hfac)_2(H_2O)$ (2.4×10^{-3})].[20] The complex with two $hfac^-$ ligands is significantly more soluble than the others, in part due to the higher fluorine content for the ligand, which makes the complex more CO_2-philic.[20,21]

(3) Relation to Gas-Phase Metal Deposition/Etching Reactions. The heterogeneous solution oxidation reactions reported herein are similar to redox transmetalation chemical vapor deposition reactions that have been extensively studied.[44−46] In these reactions, $M(hfac)_2$ acts as an oxidant for copper surfaces, and the net reaction involves the simultaneous deposition of M and etching of copper (eq 9). The $hfac^-$ ligands originally associated with the metal complex that acts as an oxidant are transferred to the copper surface. In a subsequent step, the $hfac^-$ ligands combine with oxidized copper surface atoms to produce $Cu(hfac)_2$, which desorbs from the surface at temperatures greater than 250 K. The removal of the oxidized metal from the surface by coordination to $hfac^-$ ligands is a critical reaction component for both the solution oxidative dissolution reaction and the gas-phase etching reactions.

$$M(hfac)_2 + Cu_n(s) \rightarrow MCu_{n-1}(s) + Cu(hfac)_2 \qquad (9)$$

Conclusions. These studies provide an understanding of the chemical reactions and products in a potential CO_2-based CMP process during which copper is removed in the presence of *t*-BuPA and hfacH. This work lays a foundation for converting the current aqueous/organic-based CMP technology into a "dry" CO_2-based process, by demonstrating that the *t*-BuPA/hfacH mixture is an effective etchant solution for both copper and zinc metals in nonpolar media. During the course of the oxidative dissolution reaction, no significant decomposition of hfacH is observed, and the peroxy ester cleanly undergoes reductive O−O bond cleavage to produce acetic acid and *tert*-butyl alcohol. These factors suggest that post-CMP cleaning steps may be minimized with the choice of this oxidant system. Further, the CO_2 solvent, the $M(hfac)_2$ product, and the organic products (acetic acid and *tert*-butyl alcohol) in this reaction should be recyclable, thereby reducing the environmental impact of the nonaqueous process. The generality of this reaction for dissolution of other metals and metal oxides in nonpolar solvents is currently under investigation.

Acknowledgment. We acknowledge the Kenan Center for the Utilization of CO_2 in Manufacturing and NSF-STC ROA No. 537494 for financial support. This work made use of STC shared experimental facilities supported by the National Science Foundation under Agreement No. CHE-9876674. We thank the reviewers for their insightful comments.

Supporting Information Available: Tables S1−S3 and Figures S1−S4 (PDF) and X-ray crystallographic files (CIF). This material is available free of charge via the Internet at http://pubs.acs.org.

IC049765O

(42) Rousseau, F.; Jain, A.; Kodas, T. T.; Hampden-Smith, M. J.; Farr, J. D.; Muenchausen, *J. Mater. Chem.* **1992**, *2*, 893.
(43) Droes, S. R.; Kodas, T. T.; Hampden-Smith, M. J. *Adv. Mater.* **1998**, *10*, 1129.
(44) Girolami, G. S.; Jeffries, P. M.; Dubois, L. H. *J. Am. Chem. Soc.* **1993**, *115*, 1015.
(45) Lin, W.; Wiegand, B. C.; Nuzzo, R. G.; Girolami, G. S. *J. Am. Chem. Soc.* **1996**, *118*, 5977.
(46) Lin, W.; Nuzzo, R. G.; Girolami, G. S. *J. Am. Chem. Soc.* **1996**, *118*, 5988.
(47) Obriot, J.; Ge, J.; Bose, T. K.; St-Arnaud, J.-M. *Fluid Phase Equilib.* **1993**, *86*, 315.
(48) Lemmon, E. W.; McLinden, M. O.; Friend, D. G. Thermophysical Properties of Fluid Systems. In *NIST Chemistry WebBook, NIST Standard Reference Database Number 69*; http://webbook.nist.gov.